

1-1-2012

Ultrafast dynamics of the Mn³⁺ d-d transition and spin-lattice interaction in YMnO₃ film

Z Jin

Shanghai University

Hong Ma

Shanghai University

Gaofang Li

Shanghai University

Y Xu

Shanghai University

G Ma

Shanghai University

See next page for additional authors

Follow this and additional works at: <https://ro.uow.edu.au/engpapers>



Part of the [Engineering Commons](#)

<https://ro.uow.edu.au/engpapers/5035>

Recommended Citation

Jin, Z; Ma, Hong; Li, Gaofang; Xu, Y; Ma, G; and Cheng, Zhenxiang: Ultrafast dynamics of the Mn³⁺ d-d transition and spin-lattice interaction in YMnO₃ film 2012.

<https://ro.uow.edu.au/engpapers/5035>

Authors

Z Jin, Hong Ma, Gaofang Li, Y Xu, G Ma, and Zhenxiang Cheng

Ultrafast dynamics of the Mn³⁺ d-d transition and spin-lattice interaction in YMnO₃ film

Zuanming Jin, Hong Ma, Gaofang Li, Yue Xu, Guohong Ma et al.

Citation: *Appl. Phys. Lett.* **100**, 021106 (2012); doi: 10.1063/1.3675906

View online: <http://dx.doi.org/10.1063/1.3675906>

View Table of Contents: <http://apl.aip.org/resource/1/APPLAB/v100/i2>

Published by the American Institute of Physics.

Related Articles

First-principles study of charging effect on magnetism of Pd (100) ultrathin films

J. Appl. Phys. **112**, 073910 (2012)

Magnetization of 2.6T in gadolinium thin films

Appl. Phys. Lett. **101**, 142407 (2012)

Bit error rate investigation of spin-transfer-switched magnetic tunnel junctions

Appl. Phys. Lett. **101**, 142406 (2012)

Perpendicular magnetic anisotropy of cobalt films intercalated under graphene

Appl. Phys. Lett. **101**, 142403 (2012)

Electric field assisted sputtering of Fe₃O₄ thin films and reduction in anti-phase boundaries

J. Appl. Phys. **112**, 073909 (2012)

Additional information on *Appl. Phys. Lett.*

Journal Homepage: <http://apl.aip.org/>

Journal Information: http://apl.aip.org/about/about_the_journal

Top downloads: http://apl.aip.org/features/most_downloaded

Information for Authors: <http://apl.aip.org/authors>

ADVERTISEMENT



Goodfellow
metals • ceramics • polymers • composites
70,000 products
450 different materials
small quantities fast

www.goodfellowusa.com

Ultrafast dynamics of the Mn^{3+} d-d transition and spin-lattice interaction in YMnO_3 film

Zuanming Jin,¹ Hong Ma,¹ Gaofang Li,¹ Yue Xu,¹ Guohong Ma,^{1,a)} and Zhenxiang Cheng²

¹Department of Physics, Shanghai University, 99 Shangda Road, Shanghai 200444, People's Republic of China

²Institute for Superconductor and Electronic Materials, University of Wollongong, Squires Ways, North Wollongong, New South Wales 2500, Australia

(Received 13 October 2011; accepted 19 December 2011; published online 9 January 2012)

We investigate the photo-induced carrier dynamics and spin-lattice interaction in hexagonal YMnO_3 film by the temperature-dependent femtosecond pump-probe spectroscopy. The spin-lattice interaction is identified from the slow component of the transient transmittance change with the excitation energies tuned to 1.7 eV and 2.0 eV, which are close to Mn^{3+} ions $d_{(xz),(yz)} \rightarrow d_{(z^2)}$ and $d_{(x^2-y^2),(xy)} \rightarrow d_{(z^2)}$ transition, respectively. Temperature dependences of the spin-lattice relaxation parameters demonstrate that the spin-lattice interaction is strongly connected with the d-d transition within Mn^{3+} ions and enhanced by spin ordering. © 2012 American Institute of Physics. [doi:10.1063/1.3675906]

In recent years, multiferroic oxides have attracted intense attention because of the great potential for application in the fields of oxide electronics and spintronics.¹⁻³ The physical properties of multiferroicity are extremely complicated due to the intrinsic integration and strong coupling between ferroelectricity and magnetism.^{4,5} The microscopic origin of the magnetoelectric phenomenon has been interpreted as the magnetoelastic effect,⁶ which eventually leads to an effective coupling between electric dipole moment and magnetic moment. Therefore, the understanding of the strong coupling among the charge, spin, orbital, and lattice degrees of freedom is a central topic of multiferroic oxide materials. Conventional studies of spin-lattice coupling in multiferroic oxides were investigated by steady-state spectroscopy, such as inelastic neutron scattering,⁷ Raman spectra,⁸ and thermal expansion measurements,⁹ etc. In the last two decades, ultrafast optical spectroscopy has been demonstrated to provide valuable insights into the microscopic dynamics in materials as reported in Refs. 10–16. In particular, the temperature-dependent pump-probe spectroscopy has proven to be an effective tool to study the electron-phonon, phonon-phonon, and spin-phonon interactions.¹²⁻¹⁶

Ogasawara *et al.* showed that the complex correlation between charge, lattice, and spin in various ferromagnetic and ferrimagnetic compounds can be explicitly identified from the different characteristic time scales by time-resolved magneto-optical Kerr spectroscopy (TRMOKE).¹⁰ Wall *et al.* studied the ultrafast coupling between coherent lattice vibrations and the magnetic structure of a strong spin-orbit coupling structure, LaMnO_3 .¹¹ A magnetic resonance had been observed in multiferroic $\text{Ba}_{0.6}\text{Sr}_{1.4}\text{Zn}_2\text{Fe}_{12}\text{O}_{22}$ using pump-probe reflectance spectroscopy, which revealed that the dielectric tensor of material can be modulated by magnetization precession owing to the magnetoelectric effect.¹² The intrinsic interdependence between the optical conductivity and magnetism in colossal magneto-resistance manganites $\text{La}_{0.7}\text{D}_{0.3}\text{MnO}_3$ ($\text{D} = \text{Ca}, \text{Sr}$) was investigated by Lobad

et al., which allowed for the determination of the spin-lattice coupling magnitude.^{13,14} Shih *et al.* investigated the ultrafast photoinduced electron and phonon dynamics of HoMnO_3 single crystal, and the anomalous thermoelastic effect around T_N was reported.^{15,16} These studies demonstrate that the ultrafast optical spectroscopy, even in non-Kerr experimental configurations, is an alternative method to explore the interaction of spin, charge, and lattice degrees of freedom in magnetic oxides.¹⁷

YMnO_3 in its hexagonal phase is one of the few multiferroic materials where ferroelectric and antiferromagnetic ordering coexist.¹⁸ In contrast to the other rare-earth ions in magnetic oxides, such as $\text{Ho}^{3+}(4f^{10})$, $\text{Er}^{3+}(4f^{11})$, $\text{Tm}^{3+}(4f^{12})$, and $\text{Yb}^{3+}(4f^{13})$, the magnetic properties of YMnO_3 solely originate from Mn^{3+} ions. Thus, YMnO_3 provides a pure material system for the study of interaction among charge, spin, and lattice. Hexagonal YMnO_3 is formed by stacked Mn-O and Y-O layers, in which the Mn^{3+} ions are surrounded by three in-plane and two apical oxygen ions (MnO_5 bipyramide) and form a triangular lattice. The Mn spins order antiferromagnetically below $T_N \sim 80$ K, and the spins lie in the hexagonal plane, orthogonal to the Mn-O bonds. Using optical pump-probe spectroscopy, Jang *et al.* reported a coherent 31 GHz acoustic phonon above the magnetic ordering temperature and a THz frequency coherent mode in the antiferromagnetic phase in YMnO_3 single crystals, which demonstrated that the acoustic phonon is coupled to spin ordering.¹⁹ Kimel *et al.* found that the nonlinearity in YMnO_3 results in a transient perturbation of the dielectric permittivity tensor.²⁰ Up to now, the investigation of the carrier dynamics and spin-lattice interaction in YMnO_3 film is lacking compared with HoMnO_3 and LuMnO_3 . In this letter, spin-lattice interaction in hexagonal YMnO_3 film was investigated by femtosecond pump-probe spectroscopy with varying temperature, which spans the antiferromagnetic transition temperature. Temperature dependences of the spin-lattice interaction parameters at two excitation energies reveal that the spin-lattice interaction is strongly connected with both the d-d transition within Mn^{3+} ions and the spin ordering.

^{a)}Electronic mail: ghma@staff.shu.edu.cn.

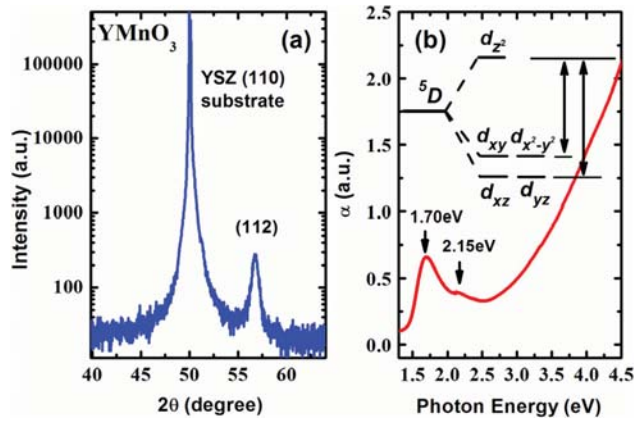


FIG. 1. (Color online) (a) XRD patterns and (b) the UV-Vis absorption spectrum for hexagonal YMnO_3 film. The inset illustrates the 3d orbit splitting of the Mn^{3+} ion in trigonal bipyramid environment.

The YMnO_3 film on YSZ (110) substrate was fabricated by a pulsed laser deposition system with a 355 nm-laser source at a repetition rate of 10 Hz. YMnO_3 targets were synthesized by a standard solid-state reaction method from the starting chemicals Y_2O_3 and MnCO_3 , with purity of 99.99%. The deposition was carried out at 800 °C with a dynamic oxygen pressure of 20 mtorr. The x-ray diffraction (XRD) pattern of the YMnO_3 film shown in Fig. 1(a) was determined with a JEOL 3500 x-ray diffractometer, which shows the YMnO_3 film is epitaxially grown on YSZ (110) with an orientation of $\langle 112 \rangle$. The inset of Fig. 1(b) shows the electronic energy diagram as derived from the local symmetry of Mn^{3+} ion.²¹ Four 3d electrons of the Mn^{3+} occupy the ground state 5D , a quintet state. In hexagonal YMnO_3 , the 5D state splits into three states under the influence of a moderate crystalline field resulting from the trigonal bipyramidal symmetry $\bar{6}m2$. Fig. 1(b) shows the room temperature absorption spectra for the hexagonal YMnO_3 film. Two absorption bands appear, a strong band around 1.70 eV and a weak one around 2.15 eV, which are attributed to inter-site optical transitions from the hybridized occupied states with $d_{(x^2-y^2),(xy)}$ and $d_{(xz),(yz)}$ orbital symmetry to the unoccupied Mn $d_{(z^2)}$ state, respectively. Charge-transfer transitions between O 2p and Mn 3d are expected to occur above 3 eV.

In time-resolved optical experiments, a pump beam excites a sample initiating a dynamical response that is monitored by a time delayed probe beam. The source of excitation consists of a mode-locked Ti:Sapphire oscillator (Mai Tai HP-1020) generating 100 fs pulses at 800 nm. A regenerative amplifier system (Spectra-Physics, Spitfire Pro)

was used to amplify the pulses 10^6 times at a repetition rate of 1 kHz. Part of the energy was used to pump an optical parametric amplifier (Topas-C) for generating different wavelengths ultrashort pulses. Pump and probe beam were focused by a 50 cm focal length lens and overlapped on the same spot of the sample with a spot size of $500 \mu\text{m}$. The ratio between the power of pump and probe beams was 50:1. The typical fluence of the pump pulses was set at $\sim 0.8 \text{ mJ/cm}^2$. The sample was mounted in a closed-cycle liquid-He cryostat in vacuum chamber with four optically accessible windows. A mechanical delay line was used to vary the arrival time of pump pulses related to probe pulses. In order to improve the immunity of laser drift, the pump beam was chopped at $\sim 490 \text{ Hz}$, and the probe signal was detected by a silicon photodiode connected to a lock-in amplifier.

Figures 2(a) and 2(b) show the typical temperature-dependent transient transmittance change ($\Delta T/T$) for the hexagonal YMnO_3 film obtained at two excitation energies, 1.70 eV and 2.0 eV, respectively. The initial rising (or falling) components of the $\Delta T/T$ indicate the Mn^{3+} d-d transition in YMnO_3 , which means the carriers transit from ground state to excited state induced by the pump pulses. The amplitudes of the initial components start to diminish around $T = 100 \text{ K}$, which is due to the Mn^{3+} d-d transition blocked when d-d transition energy level undergoes a blue-shift with decreasing temperature.^{16,22} Following the initial parts, $\Delta T/T$ curves contain three primary relaxation components: (1) the ultrafast component ($< 1 \text{ ps}$) corresponds to the electron-lattice thermalization, (2) the subsequent slow component gives a direct information of the energy exchange between the lattice and spin system, and (3) after these two relaxation processes, a quasi-constant component corresponds to either the remagnetization process or the heat diffusion out of the illuminated area of the sample. These three processes ($t > 0$) can be described by the following equation phenomenologically:

$$\Delta T/T = A \exp(-t/\tau_{fast}) + B \exp(-t/\tau_{slow}) + T_{\infty}, \quad (1)$$

where A and B are the amplitudes of the fast and slow components mentioned above, respectively. τ_{fast} and τ_{slow} are the relaxation time constant of the fast and slow components, respectively. T_{∞} is a time-independent quasi-constant parameter, which should recover to the ground state after a much longer time delay (hundreds of picoseconds—several nanoseconds). The experimental data are well fitted using the Eq. (1), which is shown in Figs. 2(a) and 2(b) as the black solid lines. Hereinafter, we focus on the discussion of

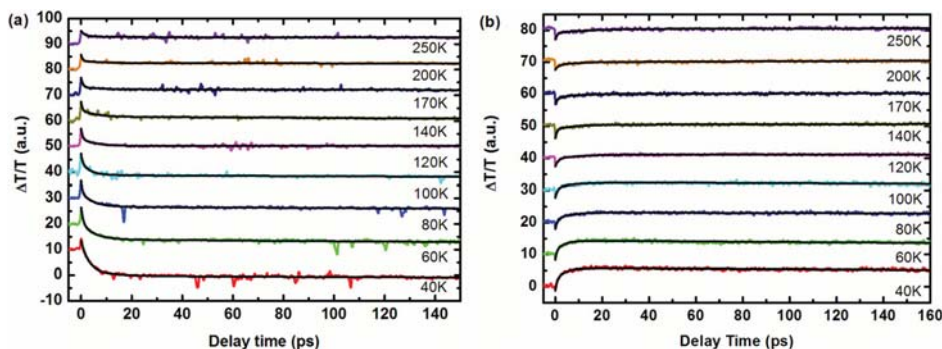


FIG. 2. (Color online) Relaxation curves of the relative transmittance change $\Delta T/T$ of YMnO_3 film at two excitation energies: (a) 1.7 eV and (b) 2.0 eV. The temperatures marked in the figure are the steady-state temperatures of sample. $\Delta T/T$ curves are shifted along the vertical axis for clarity. The black solid lines show the fitting results by Eq. (1).

temperature dependence of the slow component parameters, which is considered to relate to the spin-lattice interaction mediated by the spin-orbit coupling. The fitting fast component parameters, τ_{fast} and A, contain the information about the electron-phonon scattering, which will be discussed in another publication.²²

The main results (which are derived from the fitting data of Fig. 2) are presented in Fig. 3. Figure 3(a) shows the temperature dependences of τ_{slow} with excitation energies at 1.70 eV and 2.0 eV, respectively. The spin-lattice interaction time displays the nonmonotonic temperature dependences, and the peaks of τ_{slow} appear at ~ 120 K with values of ~ 12 ps (2.0 eV) and ~ 6 ps (1.70 eV). The observed nonmonotonic temperature dependences are indeed anticipated. Excited electrons are assumed to shed their excess energy after thermalized within the first picoseconds. A three-temperature model can be invoked to model the weak coupling between lattice and spin freedom of degrees, which is coupled by anisotropy fluctuations of the crystal field.^{23,24} The spin-lattice interaction time is related to the lattice specific heat C_l , spin specific heat C_s , and spin-lattice energy coupling constant G_{sl} as $\tau_{s-l} \approx \frac{C_l C_s}{G_{sl}(C_s + C_l)}$.^{13,24,25} Under a mean field approximation, the temperature dependent $C_s(T)$ is proportional to $\partial M^2 / \partial T$, where M is the sublattice magnetization as a function of temperature.²⁶ For weak lattice heating, the magnetic specific heat $C_s(T)$ contributes to the peak of the temperature-dependent spin-lattice relaxation time,²⁵ which was also observed in $\text{La}_{0.7}\text{Ca}_{0.3}\text{MnO}_3$ and $\text{La}_{0.7}\text{Sr}_{0.3}\text{MnO}_3$.¹³ We note here, however, the critical temperature ($T_c \sim 120$ K) is higher than the Néel temperature ($T_N \sim 80$ K) of YMnO_3 crystal, which might be caused by the short-range spin ordering. It has been reported that the short-range correlations fluctuate both in space and time above T_N in YMnO_3 . This short-range spin ordering is a signature of a spin liquid phase, which forms out of geometrically frustrated Mn moments.²⁷ It is further found that, at the temperature window from 70 to 200 K, the τ_{slow} at excitation energy of 1.70 eV is faster than that at 2.0 eV, which reveals that the spin-lattice interaction is sensitive to the photo-excitation energy. In other words, when the excitation energy

is approaching to $d_{(x^2-y^2),(xy)} \rightarrow d_{(z^2)}$ transition, the d-electrons of $(x^2 - y^2, xy)$ state could be excited, and then it will significantly affect the ordering of the Mn^{3+} spins.^{28,29} From our data, the spin-lattice coupling constant, G_{sl} , is estimated to be $\sim 75 \times 10^{10}$ and $\sim 37 \times 10^{10}$ W/(K mole) for the excitation energies of 1.7 eV and 2.0 eV, respectively. G_{sl} was calculated by taking the lattice specific heat $C_l \sim 44$ J/(K mole) and the spin specific heat $C_s \sim 5$ J/(K mole).³⁰ In addition, the lower the temperature is, in our case, lower than 70 K for 2.0 eV and 100 K for 1.7 eV, the more robust the magnetic ordering becomes due to the prevailing of the long-range antiferromagnetic ordering, as a result, a longer time is needed to disturb the spin system, which is in accordance with our observation. Similar phenomenon was also reported in HoMnO_3 single crystals.¹⁶

Figure 3(b) shows the temperature dependence of slow-component-amplitude, B, collected at the excitation energies of 1.70 eV and 2.0 eV, respectively. From our experimental results, it is expected that the intensity of the spin-lattice interaction increases markedly with decreasing temperature. We attribute this behavior to the competition between short- and long-range antiferromagnetism in YMnO_3 , which causes the significant spin-scattering behavior and then enhances the spin-lattice interaction.¹⁹

As is clearly seen in the Fig. 3(c), for excitation energy at 1.70 eV, the quasi-constant parameter T_∞ gradually decreases with decreasing temperature and alters its sign from positive to negative when temperature is approaching ~ 120 K. Nevertheless, for the excitation energy at 2.0 eV, T_∞ increases with decreasing temperature and tends to be zero above 120 K. This temperature dependence of T_∞ is relevant to the magnetism-induced redshift in the optical conductivity spectra at lower temperature.^{3,14,16,31} Ren *et al.* ascribed this long-lived component to a slow spin-relaxation process of the magnetically ordered phase in $\text{La}_{0.67}\text{Ca}_{0.33}\text{MnO}_3$.³² Shih *et al.* reported that the temperature dependence of the amplitude of the negative component is similar to the displacement of Mn atoms, which is directly related with the magnetic ordering of the Mn moments in HoMnO_3 .¹⁵

In summary, the ultrafast dynamics probed by temperature-tunable femtosecond pump-probe spectroscopy at two excitation energies are performed to investigate the spin-lattice interaction in hexagonal YMnO_3 film. Our data show that the fast component in $\Delta T/T$ corresponds to the electron-lattice thermalization, and the subsequent slow component analyzed by a three-temperature model represents the energy exchange among the electron, spin, and lattice system. Temperature dependences of slow component parameters indicate that the spin-lattice interaction in hexagonal YMnO_3 film is strongly connected with the d-d transition within Mn^{3+} ions and significantly enhanced by spin ordering.

The research is supported by National Natural Science Foundation of China (11174195) and Science and Technology Commission of Shanghai municipal (09530501100). Z. X. Cheng thanks Australia Research Council for support through a Future Fellowship.

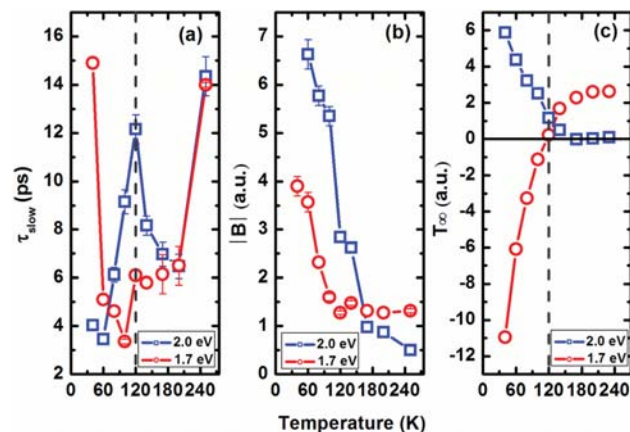


FIG. 3. (Color online) The temperature dependences of fitting parameters given by Eq. (1): (a) time constants τ_{slow} , (b) amplitudes of slow component B, and (c) background signal T_∞ for two excited energies, 1.7 eV and 2.0 eV. Vertical broken lines correspond to $T_c = 120$ K.

¹Y. Tokura, *Phys. Today* **56**(7), 50 (2003).

²J. Ma, J. Hu, Z. Li, and C.-W. Nan, *Adv. Mater.* **23**, 1062 (2011).

- ³D. N. Basov, R. D. Averitt, D. van der Marel, M. Dressel, and K. Haule, *Rev. Mod. Phys.* **83**, 471 (2011).
- ⁴C. Zhong, Q. Jiang, H. Zhang, and X. Jiang, *Appl. Phys. Lett.* **94**, 224107 (2009).
- ⁵K.-J. Jang, J. Lim, J. Ahn, J.-H. Kim, K.-J. Yee, J. S. Ahn, and S.-W. Cheong, *New J. Phys.* **12**, 023017 (2010).
- ⁶S. Lee, A. Pirogov, M. Kang, K.-H. Jang, M. Yonemura, T. Kamiyama, S.-W. Cheong, F. Gozzo, N. Shin, H. Kimura, Y. Noda, and J.-G. Park, *Nature* **451**, 805 (2008).
- ⁷S. Petit, F. Moussa, M. Hennion, S. Pailhès, L. Pinsard-Gaudart, and A. Ivanov, *Phys. Rev. Lett.* **99**, 266604 (2007).
- ⁸J. Vermette, S. Jandl, A. A. Mukhin, V. Y. Ivanov, A. Balbashov, M. M. Gospodinov, and L. Pinsard-Gaudart, *J. Phys.: Condens. Matter* **22**, 356002 (2010).
- ⁹C. dela Cruz, F. Yen, B. Lorenz, Y. Q. Wang, Y. Y. Sun, M. M. Gospodinov, and C. W. Chu, *Phys. Rev. B* **71**, 060407(R) (2005).
- ¹⁰T. Ogasawara, K. Ohgushi, Y. Tomioka, K. S. Takahashi, H. Okamoto, M. Kawasaki, and Y. Tokura, *Phys. Rev. Lett.* **94**, 087202 (2005).
- ¹¹S. Wall, D. Prabhakaran, A. T. Boothroyd, and A. Cavalleri, *Phys. Rev. Lett.* **103**, 097402 (2009).
- ¹²D. Talbayev, S. A. Trugman, A. V. Balatsky, T. Kimura, A. J. Taylor, and R. D. Averitt, *Phys. Rev. Lett.* **101**, 097603 (2008).
- ¹³A. I. Lobad, R. D. Averitt, C. Kwon, and A. J. Taylor, *Appl. Phys. Lett.* **77**, 4025 (2000).
- ¹⁴A. I. Lobad, A. J. Taylor, C. Kwon, S. A. Trugman, and T. R. Gosnell, *Chem. Phys.* **251**, 227 (2000).
- ¹⁵H. C. Shih, L. Y. Chen, C. W. Luo, K. H. Wu, J.-Y. Lin, J. Y. Juang, T. M. Uen, J. M. Lee, J. M. Chen, and T. Kobayashi, *New J. Phys.* **13**, 053003 (2011).
- ¹⁶H. C. Shih, T. H. Lin, C. W. Luo, J.-Y. Lin, T. M. Uen, J. Y. Juang, K. H. Wu, J. M. Lee, J. M. Chen, and T. Kobayashi, *Phys. Rev. B* **80**, 024427 (2009).
- ¹⁷J. S. Dodge, A. B. Schumacher, J.-Y. Bigot, D. S. Chemla, N. Ingle, and M. R. Beasley, *Phys. Rev. Lett.* **83**, 4650 (1999).
- ¹⁸H. L. Yakel, W. C. Koehler, E. F. Bertaut, and E. Forrat, *Acta Crystallogr.* **16**, 957 (1963).
- ¹⁹K.-J. Jang, H.-G. Lee, S. Lee, J. Ahn, J. S. Ahn, N. Hur, and S.-W. Cheong, *Appl. Phys. Lett.* **97**, 031914 (2010).
- ²⁰A. V. Kimel, R. V. Pisarev, F. Bentivegna, and Th. Rasing, *Phys. Rev. B* **64**, 201103(R) (2001).
- ²¹C. Degenhardt, M. Fiebig, D. Fröhlich, Th. Lottermoser, and R. V. Pisarev, *Appl. Phys. B* **73**, 139 (2001).
- ²²Y. Xu, Z. M. Jin, G. H. Ma, and Z. X. Cheng, "Ultrafast Spectroscopy of the Mn³⁺ d-d Transition on YMnO₃ Film" (unpublished).
- ²³W. Hübner and K. H. Bennemann, *Phys. Rev. B* **53**, 3422 (1996).
- ²⁴G. M. Müller, J. Walowski, M. Djordjevic, G.-X. Miao, A. Gupta, A. V. Ramos, K. Gehrke, V. Moshnyaga, K. Samwer, J. Schmalhorst, A. Thomas, A. Hütten, G. Reiss, J. S. Moodera, and M. Müntenberg, *Nature Mater.* **8**, 56 (2009).
- ²⁵Q. Zhang, A. V. Nurmikko, G. X. Miao, G. Xiao, and A. Gupta, *Phys. Rev. B* **74**, 064414 (2006).
- ²⁶D. H. Martin, *Magnetism in Solids* (MIT, Cambridge, MA, 1967).
- ²⁷J. Park, J.-G. Park, G. S. Jeon, H.-Y. Choi, C. Lee, W. Jo, R. Bewley, K. A. McEwen, and T. G. Perring, *Phys. Rev. B* **68**, 104426 (2003).
- ²⁸T. Katsufuji, S. Mori, M. Masaki, Y. Moritomo, N. Yamamoto, and H. Takagi, *Phys. Rev. B* **64**, 104419 (2001).
- ²⁹K. Murakami, T. Yamauchi, A. Nakamura, Y. Moritomo, H. Tanaka, and T. Kawai, *Phys. Rev. B* **73**, 180403(R) (2006).
- ³⁰D. G. Tomuta, S. Ramakrishnan, G. J. Nieuwenhuys, and J. A. Mydosh, *J. Phys.: Condens. Matter* **13**, 4543 (2001).
- ³¹R. C. Rai, J. Cao, J. L. Musfeldt, S. B. Kim, S.-W. Cheong, and X. Wei, *Phys. Rev. B* **75**, 184414 (2007).
- ³²Y. H. Ren, M. Ebrahim, H. B. Zhao, G. Lüpke, Z. A. Xu, V. Adyam, and Q. Li, *Phys. Rev. B* **78**, 014408 (2008).